Lasers in Manufacturing Conference 2019

Correlation of Spatter Formation and Process Parameters during Selective Laser Melting of AlSi10Mg

Artur Leis[a,b*], Lukas Voltin[b], Rudolf Weber[b], Thomas Graf[b]

[a]*Graduate School of Excellence advanced Manufacturing Engineering (GSaME), Nobelstraße 12, 70569 Stuttgart, Germany*
[b]*Institut für Strahlwerkzeuge (IFSW), Pfaffenwaldring 43, 70569 Stuttgart, Germany*

Abstract

The spatter formation was investigated in a model arrangement by means of high-speed imaging with a frame rate up to 10,000 fps. The process parameters laser power and feed rate were varied in order to adjust the line energy.
The correlation of the spatter formation and the process parameters was investigated. Advantageous parameter ranges with significantly decreased spatter formation, quantified by the mean ejection angle and the number of spatters, will be presented in this proceeding.

Keywords: selective laser melting, SLM, additive manufacturing, Spatter formation, process diagnostics, AlSi10Mg

1. Introduction

Selective laser melting (SLM) is a powder bed based additive manufacturing process, which is able to produce parts with high geometrical complexity due to layer wise melting as discussed by Adam, 2015 and Olakanmi et al., 2015. The formation of spatters, pores and cracks during the SLM process reduce the quality of the parts. For example, Bidare et al., 2018 have shown that gas expansion accelerates the single powder particles, which results in a particle flight. Also molten and fused particles may be ejected out of the interaction area of the laser and the material as shown by Parab et al., 2018, Özel et al., 2018 and Lutter-Günther et al., 2018. Furthermore, spatters with large ejection angles may interact with the laser beam during their flight, presented by Guo et al., 2018, or in general within the following layer as investigated by Liu et al., 2015. The size of the solidified spatters differs from the size of the powder particles. A high number

* Corresponding author. Tel.: +49 711 685 60428; fax: +49 711 66842
E-mail address: artur.leis@ifsw.uni-stuttgart.de

of ejected spatters can result in a decrease of generated material for each layer. Additionally, solidified spatters lead to the generation of inhomogeneous layers and therefore in geometrical deviations of the generated parts as presented by Liu et al., 2015. Therefore, decreasing the number of ejected spatters and powder particles as well as a low ejection angles are mandatory during SLM, in order to reduce the number of the defects of a part. From conventional laser beam welding it is known, that the feed rate has a major influence on the characteristics of the generated spatters, as shown by Weberpals, 2010.

In this proceeding, the influence of the feed rate and the laser power on the number of spatters and their ejection angle during the SLM process is described.

2. Experimental setup and evaluation procedure

The experimental setup is shown in Fig. 1 a). A simplified powder bed was used for the investigation of the mean ejection angle and the number of spatters at varying process parameters. The feed was generated by the movement of the sample. This allowed for better accessibility of the process diagnostics. The feed direction of the sample is shown by the black arrows. Nitrogen was used as shielding gas. A high-speed camera was placed parallel to the sample's surface and perpendicular to the laser beam and feed direction. The process was illuminated with a diode laser with a wavelength of 808 nm. Images were recorded with 10,000 fps using a band pass filter for the illuminating wavelength. A TruDisk 8001 was used as process laser. The laser focus diameter was 100 µm, focused on top of the sample surface. A schematic illustration for reproducible generation of powder layers is shown in Fig. 1 b). Adjusting sheets with a thickness of 50 µm allowed to generate powder layers with a homogeneous thickness. Trumpf AlSi10Mg-A LMF powder was used.

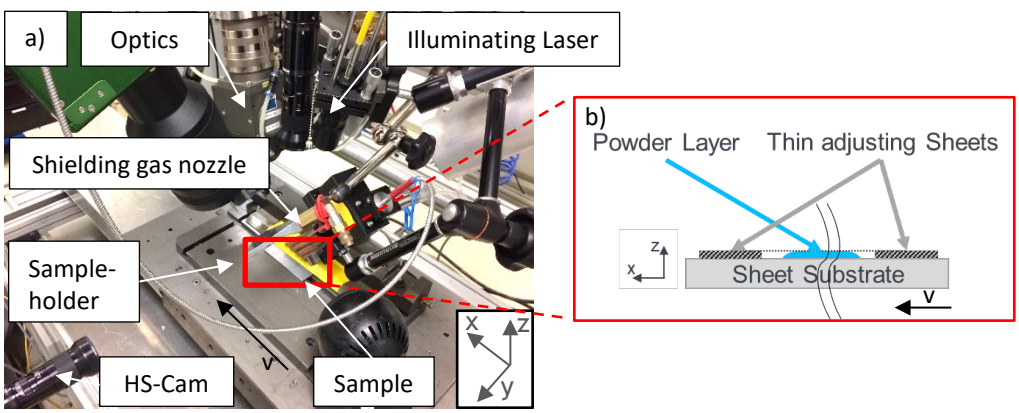

Fig. 1. a): Simplified powder bed for investigating the moving sample, b): Schematic illustration for reproducible generation of powder layers.

The mean ejection angle and the number of ejected spatters were determined. For this, high-speed images were processed with the Fiji plugin TrackMate published by Tinevez et al., 2017. The process was analyzed after reaching steady state condition during processing of a distance of 10 mm. In Fig. 2, an exemplary average image of recorded high-speed images is shown. The trajectories of the spatters were tracked with TrackMate. The yellow lines show the single spatter trajectories in the x-z-plane beginning at the interaction area of the sample and the laser beam.

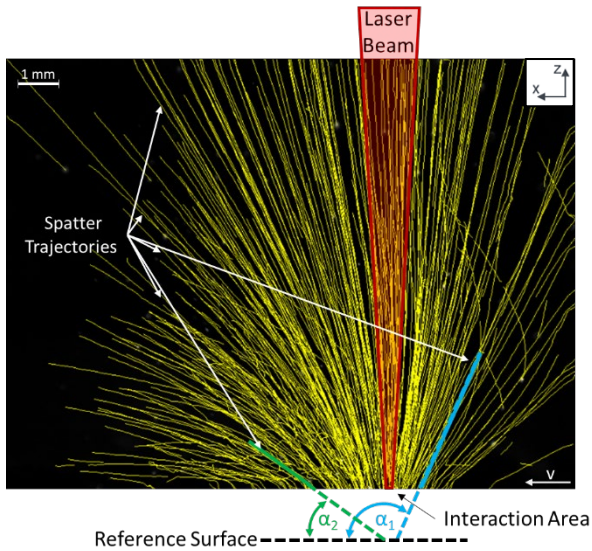

Fig. 2. Average image of a recorded high-speed video with trajectories of spatters tracked with Fiji TrackMate for P = 500 W and v = 0.5 m/s. Two exemplary trajectories are highlighted in blue and green lines. These show the ejection angles in relation to the reference surface. The shown feed direction v is the moving direction of the sample.

The blue and green lines describe two exemplary trajectories and their corresponding ejection angles α_1 and α_2. The reference surface is a projection of the sample surface and represented by the dashed black line. The feed direction of the sample is shown by the white arrow in the down right.

Ejection angles larger than 85° lead to an interaction of the flying spatters with the laser beam. This is shown by the displayed laser beam in Fig. 2. This leads to a partial absorption of the laser beam above the melt pool, which influences the interaction area. Defects and inhomogeneities occur in the generated parts.

From the trajectories we can determine two quantities for the validation of the process. First the total number of spatters n, which results from the number of trajectories captured within 10 mm. Second the ejection angle α_i of the individual spatters. This results in the mean ejection angle

$$\bar{\alpha} = \frac{1}{n}\sum_{i=1}^{n} a_i \qquad (1)$$

with the ratio of the sum of the ejection angles α_i of individual spatters and the total number of the spatters n captured within 10 mm.

3. Results

Fig. 3 shows average images of high-speed images for different feed rates and laser powers with the trajectories of the ejected spatters tracked with TrackMate as described in Fig. 2. Both, the average power and the feed rate are increasing from left to right. The line energy is kept constant at 1000 J/m. In Fig. 3 a) two different key ranges of ejection angles can be seen, whereby in Fig. 3 b) the individual ejection angles are uniformly distributed in the range from 10° to 155°. Furthermore, a significant decrease of the ejection angle occurs in case of increasing the velocity from 0.5 m/s (Fig. 3 b)) to 1 m/s (Fig. 3 c)). A further increase of the average power and feed rate leads to increased ejection angles as shown in Fig. 3 d). Spatters with a

larger ejection angle α_i than 85° in relation to the reference surface, e.g. in Fig. 3 a), b) and d), lead to the interaction of the spatters with the laser beam during their flight. In Fig 3 c) the interaction of the ejected spatters and the laser beam is reduced to a minimum.

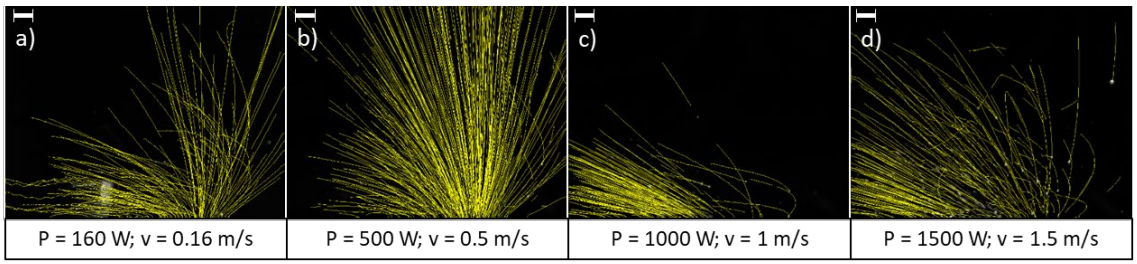

Fig. 3. Average images of recorded high-speed images with trajectories of spatters tracked with Fiji TrackMate for identical line energies of 1000 J/m. The shown scale bar is 1000 µm at each image.

The average number of spatters per unit length over four measurements is shown in Fig. 4 a). It is lowest at the lowest feed rate. With increasing feed rate, the number of spatters reaches a local maximum at 0.4 - 0.5 m/s and decrease at 0.8 - 1 m/s to the local minimum, except for 250 J/m. Further increase of the feed rate leads again to a higher number of spatters.

Fig. 4 b) shows the mean ejection angle $\bar{\alpha}$ of the spatters averaged over four measurements as a function of the feed rate for different line energies. At feed rates below 0.75 m/s the mean ejection angle $\bar{\alpha}$ is larger than 40° at each analyzed line energy. With increasing feed rate, the mean ejection angle $\bar{\alpha}$ is decreasing for line energies above 500 J/m to approximately 20°. The mean ejection angle $\bar{\alpha}$ at line energy of 250 J/m is increasing with increasing feed rate up to 1.25 m/s to 50°, then decreasing again to 30°. At 500 J/m the mean ejection angle $\bar{\alpha}$ is increasing up to 73° at 0.625 m/s and decreasing to 52° at 0.8 m/s. The length of the error bars in Fig. 4 a) and b) represent the range between the minimum and maximum measured values out of four measurements.

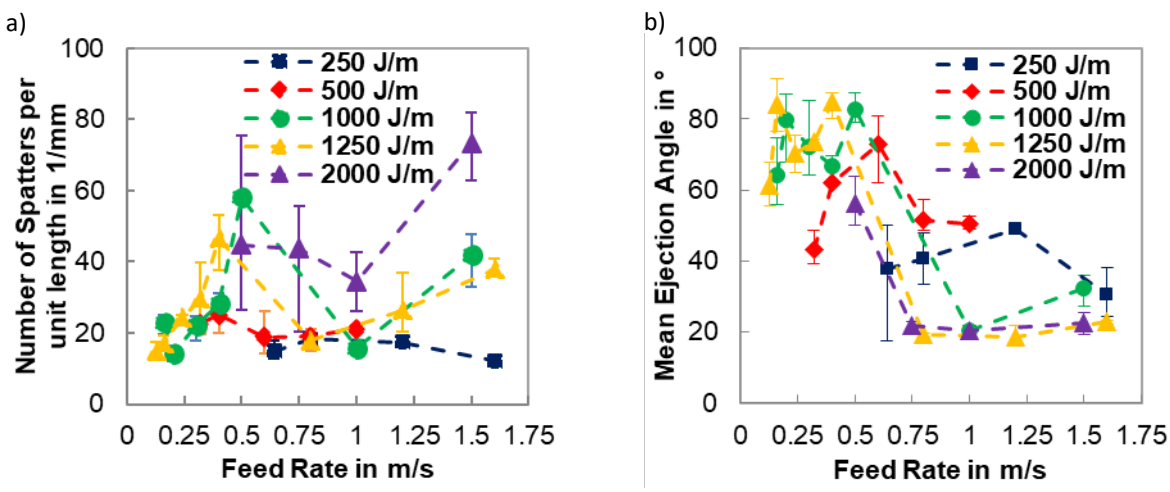

Fig. 4. a): Number of spatters per unit length in dependence of the feed rate for different line energies, b): Mean ejection angle $\bar{\alpha}$ as a function of the feed rate for different line energies.

4. Conclusion

Selective laser melting with feed rates above 1.25 m/s leads to an increased number of spatters per unit length, which influences the following layers and generate inhomogeneous layers. Feed rates below 0.6 m/s leads to large ejection angles. This allows an interaction of the spatters with the laser beam during their flight. An optimum parameter range was identified: The reduced number of spatters and the reduced mean ejection angles reveal that the favorable feed rate is between 0.75 m/s and 1.25 m/s essentially independent of the line energy.

References

Adam G. A. O., 2015. Systematische Erarbeitung von Konstruktionsregeln für die additiven Fertigungsverfahren Lasersintern, Laserschmelzen und Fused Deposition Modeling. Dissertation

Bidare P., Bitharas I., Ward R. M., Attallah M. M., Moore A. J., 2018. Fluid and particle dynamics in laser powder bed fusion. Acta Materialia 142, pp 107–120. doi: 10.1016/j.actamat.2017.09.051

Guo Q., Zhao C., Escano L. I., Young Z., Xiong L., Fezzaa K., Everhart W., Brown B., Sun T., Chen L., 2018. Transient dynamics of powder spattering in laser powder bed fusion additive manufacturing process revealed by in-situ high-speed high-energy x-ray imaging. Acta Materialia 151, pp 169–180. doi: 10.1016/j.actamat.2018.03.036

Liu Y., Yang Y., Mai S., Di Wang, Song C., 2015. Investigation into spatter behavior during selective laser melting of AISI 316L stainless steel powder. Materials & Design 87, pp 797–806. doi: 10.1016/j.matdes.2015.08.086

Lutter-Günther M., Bröker M., Mayer T., Lizak S., Seidel C., Reinhart G., 2018. Spatter formation during laser beam melting of AlSi10Mg and effects on powder quality. Procedia CIRP 74, pp 33–38. doi: 10.1016/j.procir.2018.08.008

Olakanmi E. O., Cochrane R. F., Dalgarno K. W., 2015. A review on selective laser sintering/melting (SLS/SLM) of aluminium alloy powders: Processing, microstructure, and properties. Progress in Materials Science 74, pp 401–477. doi: 10.1016/j.pmatsci.2015.03.002

Özel T., Shaurya A., Altay A., Yang L., 2018. Process monitoring of meltpool and spatter for temporal-spatial modeling of laser powder bed fusion process. Procedia CIRP 74, pp 102–106. doi: 10.1016/j.procir.2018.08.049

Parab N. D., Zhao C., Cunningham R., Escano L. I., Fezzaa K., Everhart W., Rollett A. D., Chen L., Sun T., 2018. Ultrafast X-ray imaging of laser-metal additive manufacturing processes. J Synchrotron Radiat 25, pp 1467–1477. doi: 10.1107/S1600577518009554

Tinevez J.-Y., Perry N., Schindelin J., Hoopes G. M., Reynolds G. D., Laplantine E., Bednarek S. Y., Shorte S. L., Eliceiri K. W., 2017. TrackMate: An open and extensible platform for single-particle tracking. Methods 115, pp 80–90. doi: 10.1016/j.ymeth.2016.09.016

Weberpals J.-P. (2010). Nutzen und Grenzen guter Fokussierbarkeit beim Laserschweißen. Zugl.: Stuttgart, Univ., Diss., 2010. Laser in der Materialbearbeitung. Utz, München